Vehicular Communications 2 (2015) 47–57

Contents lists available at ScienceDirect

Vehicular Communications

www.elsevier.com/locate/vehcom

Irresponsible AODV routing ☆

Andrea Gorrieri *, Gianluigi Ferrari **

Wireless Ad-hoc Sensor Network Laboratory, Department of Information Engineering, University of Parma, I-43124, Parma, Italy

A R T I C L E I N F O

Article history:
Received 10 July 2014
Received in revised form 15 December 2014
Accepted 22 January 2015
Available online 16 February 2015

Keywords:
Vehicular Ad-hoc NETwork (VANET)
Pedestrian networks
Ad-hoc On demand Distance Vector (AODV) routing
Flooding
Broadcast
Forwarding

A B S T R A C T

Broadcasting is a common transmission strategy used by several ad-hoc routing protocols in order to solve many issues, such as finding a route to a new host or sending control messages to all nodes in the network. Flooding is the simplest technique to achieve broadcast communications and it is widely used in many existing routing protocols for Mobile Ad-hoc NETworks (MANETs). However, because of multiple access interference, due to redundant transmissions, flooding tends to be inefficient. In this paper, the well-known Ad-hoc On demand Distance Vector (AODV) routing protocol [1] is modified by replacing the flooding mechanism, used in its route discovery process, with the probabilistic forwarding technique given by Irresponsible Forwarding (IF) [2]. The performance of the new routing protocol, denoted as *irresponsible* AODV (iAODV), is analyzed in three characteristic scenarios (pedestrian, pedestrian–vehicular, and vehicular). The obtained results show that the iAODV protocol can outperform the AODV protocol by significantly reducing the overhead traffic during the route discovery phase. This is more pronounced the higher are the node spatial density and/or data traffic load. The impact, on the system performance, of fundamental network parameters is investigated.

1. Introduction

A Mobile Ad-hoc NETwork (MANET) consists of a set of mobile devices that communicate dynamically without the need of a pre-existing network infrastructure. In a MANET, each node may forward data packets associated with multi-hop communications between other pairs of nodes, so that each node can act as source, rebroadcaster, and destination at the same time. MANETs can be useful in all situations where networks need to be deployed very quickly and fixed network infrastructures are not available. Due to the growing interest in smart cities and Internet of Things (IoT) applications [3], in the last years subclasses of MANETs, such as Vehicular Ad-hoc NETworks (VANETs) [4] and Opportunistic (such as pedestrian or Machine-to-Machine, M2M) ad-hoc networks [5], have been intensely investigated. In this type of networks, nodes share a common channel and can be highly mobile, thus making the design of routing protocols very challenging.

The scientific community has tackled the design of multi-hop communication protocols very intensely in the past decade, and many routing protocols for ad-hoc networks have been proposed and analyzed [6,7]. Although these protocols tend to be very different from each other, they all typically rely on flooding mechanisms in order to perform some routing operations, such as finding a route to a desired destination or sending control messages to all nodes in the network. This is especially true for reactive routing protocols, such as Ad-hoc On-demand Distance Vector (AODV) [1] and Dynamic Source Routing (DSR) [8], which utilize flooding in the so-called "route discovery" phase. The flooding strategy can be very inefficient in MANETs and, because of highly redundant transmissions, can lead to serious inefficiencies, caused by collisions and interference. This problem, referred to as Broadcast Storm Problem (BSP) [9], is more exacerbated the higher are the node spatial density, the node mobility level, and/or the data traffic load.

In general, there are many approaches that can be used in order to reduce the redundancy introduced by flooding—the interested reader is referred to [9] for a possible classification—and, thus, design energy-efficient broadcast mechanisms. One possibility is to adopt a probabilistic broadcasting approach. According to this approach, a potential rebroadcaster node retransmits a packet with probability p and, consequently, takes no action with probability $1 - p$. According to the probabilistic forwarding strategy, denoted as Irresponsible Forwarding (IF), introduced in [2], a node computes the retransmission probability for each received packet taking into account the node spatial density, the transmission range (assumed fixed for all nodes), and the distance from the transmitter.

☆ The work of Andrea Gorrieri is partially supported by the SPINNER 2013.
* Principal corresponding author.
** Corresponding author.
E-mail addresses: andrea.gorrieri@gmail.com (A. Gorrieri), gianluigi.ferrari@unipr.it (G. Ferrari).

http://dx.doi.org/10.1016/j.vehcom.2015.01.002
2214-2096/

In this work, we propose a novel reactive routing protocol, denoted as irresponsible AODV (iAODV), obtained from the AODV protocol by replacing, in the route discovery process, the flooding mechanism with IF. In order to exhaustively investigate the performance of the iAODV protocol, three different types of scenarios are considered: (i) pedestrian, (ii) pedestrian–vehicular, and (iii) vehicular. The results show that the iAODV protocol outperforms (in terms of throughput and delay) the AODV protocol in all scenarios and in almost all considered network conditions, especially for high traffic load and/or high node spatial density. Moreover, owing to the use of IF in the route discovery process, the iAODV protocol can adapt effectively its behavior to the network conditions.

The remainder of this paper is organized as follows. In Section 2, we provide an overview of related work, with focus on the mitigation of the BSP. In Section 3, the IF technique is briefly recalled. In Section 4, the iAODV protocol is introduced: first, a brief overview of the AODV protocol is provided, focusing on the use of flooding in the route discovery process; then, we describe how the IF strategy is embedded into the route discovery process, leading to iAODV; finally, the capability of the iAODV protocol to mitigate the BSP is analytically evaluated. In Section 5, the three scenarios of interest (pedestrian, pedestrian–vehicular, and vehicular) are described. In Section 6, the performance of the iAODV protocol, directly compared with that of the AODV protocol, is investigated in the considered scenarios. Finally, Section 7 concludes the paper.

2. Related work

In [10], authors explore the so-called "phase transition" phenomenon as a basis for defining probabilistic flooding. A phase transition occurs when a generic network parameter p exceeds a certain threshold value p_c, denoted as "critical point," radically changing the overall behavior of the network. In particular, in [10] the parameter p corresponds to the retransmission probability, which is considered fixed and equal for all nodes in network.

The phase transition phenomenon for a probabilistic broadcast technique is analyzed also in [11] where the authors show that replacing flooding with probabilistic broadcast in the route discovery process of the AODV protocol brings a significant performance improvement. In particular, for large networks, the number of control messages used by the modified AODV protocol, denoted as AODV+G, reduces by 35% with respect to that of the AODV protocol. In [11], as in [10], probabilistic flooding is performed with a fixed retransmission probability, which is the same in all network conditions and does not depend on the specific values of network parameters. In both [10] and [11], the concept of percolation [12,13] is used to characterize the phase transition.

In [14], the authors focus on the problem of the construction of a broadcast communication tree, defined as the set of nodes involved in a packet forwarding process—the set includes sources, relays, and destinations. In [14], several algorithms for broadcast communication tree construction in infrastructureless networks are proposed and analyzed. In particular, these algorithms, exploiting the characteristics of the wireless medium, create broadcast transmission trees that are optimal in terms of energy consumption minimization.

According to a completely different point of view, in [15] the authors analyze a physical layer cooperative flooding scheme. The idea is that while at the network layer collisions are harmful, at the physical layer broadcast messages can cooperate thus increasing the received power and the transmission range. This approach is in contrast with the traditional network layer flooding, that treats each link individually and attempts to eliminate collisions as much as possible.

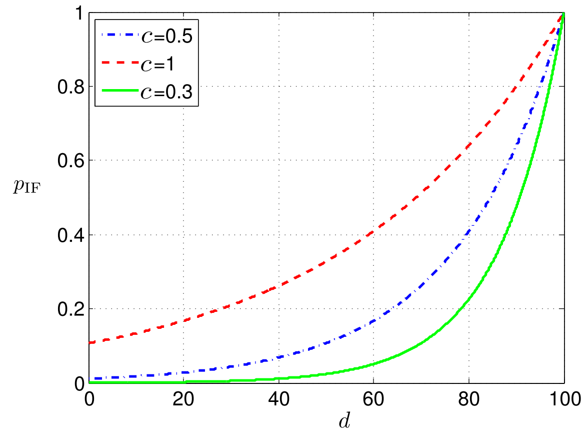

Fig. 1. IF PAF, as a function of the internode distance, for various values of the shaping parameter c. In all cases, $\rho = 900$ nodes/km^2 and $z = 100$ m.

3. Irresponsible forwarding

IF is a probabilistic forwarding technique in which every node computes its own retransmission probability in a per-packet manner. In a single source scenario, the broadcast forwarding process of IF can be summarized as follows: the initial transmission of a new packet from the source is denoted as the 0-th hop transmission. The packet is then received by all the source neighbors, that are the potential rebroadcasting nodes for the 1-st hop. Hence, their union constitutes the "1-st transmission domain." Each node of the 1-st transmission domain rebroadcasts, independently from the other nodes of the same domain, with a probability computed according to a proper Probability Assignment Function (PAF). The nodes receiving a packet from the rebroadcasters of the 1-st transmission domain constitute the 2-nd transmission domain and some of them rebroadcast according to the PAF previously mentioned. The process then repeats itself recursively.

Intuitively, the farther the potential rebroadcaster node is from the transmitting node, the higher its associated rebroadcast probability should be, as this will yield the highest forward progress. Based on this idea, in [2] the PAF of IF is introduced for a monodimensional scenario (e.g., narrow street). In a realistic bidimensional scenario (e.g., a city square), the PAF of IF can be generalized as follows:

$$p_{\rm IF} = \exp\left\{-\frac{\sqrt{\rho}(z-d)}{c}\right\} \tag{1}$$

where: d is the distance between the transmitter and a potential rebroadcaster (dimension: [m]); z is the transmission range (dimension: [m]); c is a shaping coefficient (adimensional) which can be used in order to tune the retransmission probability [16]; ρ is the bidimensional nodes spatial density (dimension: [nodes/km^2]). According to the PAF (1), if the network is sparse, the overall retransmission probability is high, so that complete connectivity can still be guaranteed; on the other hand, if the network is spatially dense, the overall retransmission probability is low in order to limit transmission redundancy and collisions. In Fig. 1, the PAF (1) is shown as a function of the internode distance d for three different values of c. The node spatial density ρ is set to 900 nodes/km^2 and the transmission range z is set to 100 m.

The idea behind the IF rebroadcasting paradigm is that once a node receives a packet, it estimates, in an average statistical sense, the presence of other nodes in its proximity. If the probability that another node can rebroadcast the packet is sufficiently high, then the node of interest "irresponsibly" chooses not to rebroadcast. In [2,16], it is shown that this irresponsible approach becomes very beneficial for increasing traffic load and/or node spatial density.

Since IF is based on the assumption of knowing the values of some topological network parameters—such as internode distance and node spatial density—in this work we assume that each node is equipped with a Global Positioning System (GPS) interface. This allows a receiving node to evaluate the distance from the transmitting node. Moreover, each node could estimate the local node spatial density ρ by evaluating the distances of its direct neighbors.

4. Embedding IF into AODV

In this section, we first provide an overview of the AODV protocol, focusing on when and how flooding is performed. Then, we show how the IF strategy can be embedded into the AODV protocol. Finally, the ability of the iAODV protocol to mitigate the BSP is quantified analytically.

4.1. The AODV routing protocol

The AODV protocol, derived from the Distance Vector (DV) protocol [17], is one of the most sought routing protocols for ad-hoc networks. AODV is a *reactive* routing protocol: this means that a source node tries to find a multi-hop route to a desired destination node only when it has packets to transmit. No control or routing information is generated by nodes that are not involved in a communication. This kind of approach is opposed to the *proactive* one, such as that used by the Destination Sequenced Distance Vector (DSDV) protocol [18]. With a proactive approach, all nodes in the network update their routing tables by regularly exchanging control messages. Although this strategy allows to maintain up-to-date routing information from each node to every other node, it leads to a constant overhead of routing traffic. However, no initial delay is required in order to discover the route to the destination.

Unlike proactive protocols, with the AODV protocol a source node, which does not have any routing information about a desired destination in its routing table, first performs a so-called "route discovery" process, based on pure flooding, which can be described as follows. The source node transmits to its neighbors a Route REQuest (RREQ) packet, which contains the destination address and some other information, such as a *broadcast id* and a *hop counter*. A neighbor replies to the source with a Route REPly (RREP) message if it has routing information related to the destination; otherwise, the neighbor rebroadcasts the RREQ increasing the hop counter.

One basic feature of the AODV protocol is the use of the so-called destination sequence number. This number is periodically generated by each node in order to maintain the entries of the routing tables "fresh." Should a requesting node have the possibility of choosing between two routes to a destination, the one associated with the largest sequence number would be selected.

Another important property of the AODV protocol is the management of the local connectivity. If a node does not send a message to any of its neighbors within a *hello interval* (dimension: [s]), it broadcasts a special RREP, denoted as *hello message*, containing its identity. The *hello message* is not further rebroadcasted by the node's neighbors because its field *Time To Live* (TTL) is set to 1. Hello messages are used to detect a route break as follows: if a relay node between a source and a destination fails to receive a minimum number, denoted as *allowed hello loss*, of hello messages from the next hop in the path, a notification of link failure is sent to the source. In this case, another route discovery process is required and a new "wave" of RREQ messages floods the network. For this reason, hello messages and, in particular, the values of the parameters *hello interval* and *allowed hello loss* have a significant impact on the total number of transmitted RREQ packets.

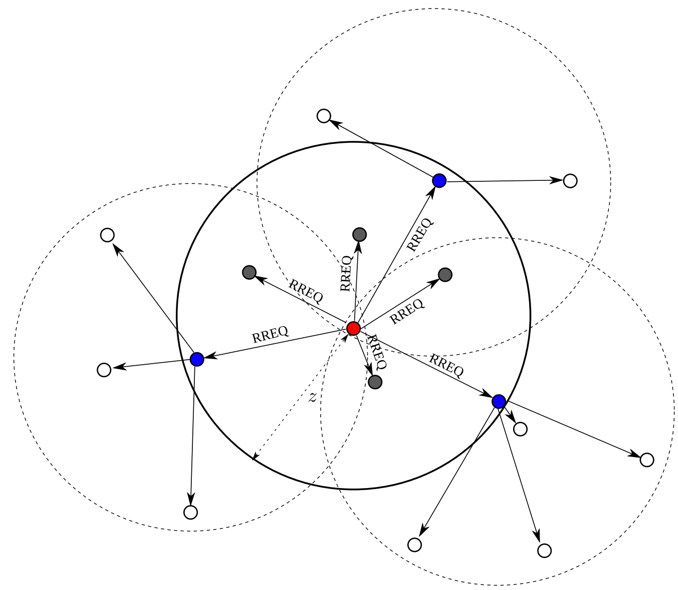

Fig. 2. Illustrative example of iAODV route discovery process. Nodes which are far away from the source rebroadcast the RREQ with higher probability.

4.2. IF in the route discovery process

In order to limit the number of broadcasted RREQ packets and, consequently, the BSP, we propose to replace the flooding mechanism, used in the route discovery process of AODV, with IF. When a node receives an RREQ packet, it first checks its *broadcast id*: if it has already received another RREQ packet with the same *broadcast id*, the redundant RREQ packet is dropped; if this is not the case and if the node has no routing information to the destination, the RREQ packet is rebroadcasted with a probability given by (1). This new variant of the AODV protocol will be referred to as iAODV. In Fig. 2, an illustrative example of the iAODV route discovery process is shown: according to the IF principle, the RREQs are propagated only (in a statistical sense) by the farthest nodes in the 1-st transmission domain.

4.3. BSP mitigation: an analytical evaluation

In order to measure the capability of the iAODV protocol to mitigate the BSP, we analytically evaluate the number of saved redundant rebroadcasts brought by the use of IF in the route discovery phase of iAODV. While a similar analysis is carried out in [2] for a monodimensional scenario, in the following we consider a more realistic bidimensional scenario—this is more relevant for pedestrian, rather than vehicular, networks.

Let us consider the first rebroadcast round as shown in Fig. 2, where the source node is placed in the center of its circular coverage area (with radius z) and transmits to all its neighbors the first RREQ packet. We denote the total number of rebroadcasts in this first rebroadcast round as N_{rtx}. The total number of nodes in the coverage area (i.e., the source neighbors) is, on average, the following:

$$\overline{N}_z = \rho \pi z^2. \tag{2}$$

According to the IF strategy, some of the neighbor nodes will rebroadcast the RREQ packet, while the others will be inhibited from doing it. Denoting with Γ the random variable "retransmission probability of a neighbor node" (obviously, $\Gamma \in [0, 1]$), under the use of the IF protocol the average number of rebroadcasts in the first round can be written as follows:

$$\overline{N}_{\text{rtx-IF}} = \rho \pi z^2 \mathbb{E}\{\Gamma\} \tag{3}$$

where:

$$\mathbb{E}\{\Gamma\} = \int_{-\infty}^{\infty} \gamma\, f_\Gamma(\gamma)\, \mathrm{d}\gamma = \int_0^1 \gamma\, f_\Gamma(\gamma)\, \mathrm{d}\gamma \tag{4}$$

and $f_\Gamma(\gamma)$ is the Probability Density Function (PDF) of Γ. Denoting as D the random variable representing the "distance between the source node and one of its neighbor," by applying the total probability theorem [19], $f_\Gamma(\gamma)$ can be rewritten as follows:

$$f_\Gamma(\gamma) = \int_0^z f_\Gamma(\gamma|D=\delta)\, \mathbb{P}\{D=\delta\}\, \mathrm{d}\delta = \int_0^z f_\Gamma(\gamma|D=\delta)\, f_\mathrm{D}(\delta)\, \mathrm{d}\delta \tag{5}$$

where $f_\mathrm{D}(\delta)$ is the PDF of D. By replacing (5) into (4), one obtains:

$$\begin{aligned}\mathbb{E}\{\Gamma\} &= \int_0^1 \gamma \int_0^z f_\Gamma(\gamma|D=\delta)\, f_\mathrm{D}(\delta)\, \mathrm{d}\delta\, \mathrm{d}\gamma \\ &= \int_0^z \int_0^1 \gamma\, f_\Gamma(\gamma|D=\delta)\, f_\mathrm{D}(\delta)\, \mathrm{d}\gamma\, \mathrm{d}\delta. \end{aligned} \tag{6}$$

The PDF of Γ, conditioned to the fact that the neighbor node is at a distance δ from the source, is a Dirac delta function, i.e.,

$$f_\Gamma(\gamma|D=\delta) = \begin{cases} 1 & \text{if } \gamma = e^{-\frac{(z-\delta)}{c}\rho} \\ 0 & \text{otherwise.} \end{cases} \tag{7}$$

Using (7) into (6) one obtains:

$$\mathbb{E}\{\Gamma\} = \int_0^z e^{-\frac{(z-\delta)}{c}\rho}\, f_\mathrm{D}(\delta)\, \mathrm{d}\delta \tag{8}$$

In order to find an expression for $f_\mathrm{D}(\delta)$, it is convenient to define a coordinate system where the source node is placed at the origin, so that $\mathcal{C} \triangleq \{(x,y) \in \mathbb{R}^2 : x^2 + y^2 \le z^2\}$ represents the set of coordinates within the coverage area of the source. Defining $\mathcal{E} \triangleq \{(x,y) \in \mathbb{R}^2 : x^2 + y^2 \le \delta^2\}$, the Cumulative Density Function (CDF) of D, denoted as $F_\mathrm{D}(\delta)$, can be expressed as the fraction between the area of the region identified by $\mathcal{E}$ and the coverage area, i.e.:

$$F_D(\delta) = \mathbb{P}\{D \le \delta\} = \frac{\pi\delta^2}{\pi z^2} = \left(\frac{\delta}{z}\right)^2. \tag{9}$$

Therefore,

$$f_D(\delta) = \frac{\mathrm{d}F_D(\delta)}{\mathrm{d}\delta} = \frac{2\delta}{z^2}. \tag{10}$$

By replacing (10) into (8), the average retransmission probability with IF can be expressed as follows:

$$\mathbb{E}\{\Gamma\} = \frac{2}{z^2} e^{-\frac{z\rho}{c}} \int_0^z \delta e^{\frac{\delta\rho}{c}}\, \mathrm{d}\delta = \frac{2c}{z\rho}\left[1 + \frac{c}{z\rho}\left(e^{-\frac{z\rho}{c}} - 1\right)\right]. \tag{11}$$

Finally, by replacing (11) into (3) one obtains the following expression for the average number of rebroadcasters in the first rebroadcast domain:

$$\overline{N}_{\text{rtx-IF}} = 2\pi c\left[z + \frac{c}{\rho}\left(e^{-\frac{z\rho}{c}} - 1\right)\right]. \tag{12}$$

Note that, as a consistency check, for $c \to \infty$ it follows that the right-hand side in (12) tends to the average number of transmissions in the first broadcast round with the flooding protocol, i.e.:

$$\lim_{c\to+\infty} \overline{N}_{\text{rtx-IF}} = \lim_{c\to+\infty} 2\pi c\left[z + \frac{c}{\rho}\left(e^{-\frac{z\rho}{c}} - 1\right)\right] = \pi z^2 \rho \tag{13}$$

where the limit follows observing that the second-order Taylor series expansion of the term $\exp(-(z\rho)/c)$ is equal to $(1 - (z\rho)/c + (z\rho)^2/2c^2$. We remark that, since with the flooding protocol each neighbor node rebroadcasts the RREQ packet, the average number of rebroadcasters is equal to $\overline{N}_\mathrm{z}$ given by (2).

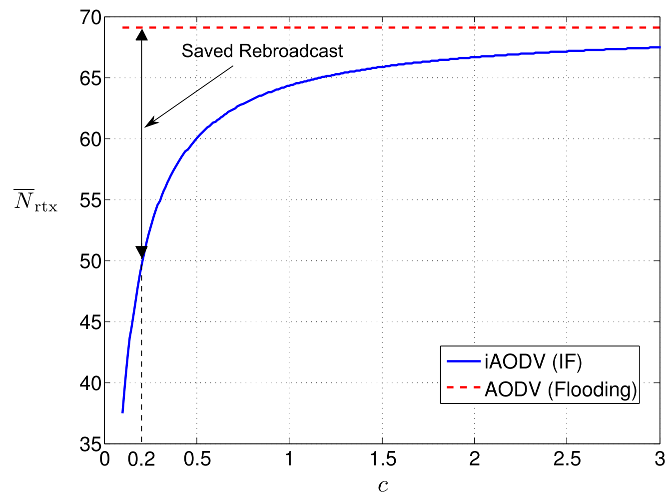

Fig. 3. Average number of retransmissions, in the first rebroadcast round of the route discovery phase, as a function of c. The performance of iAODV (with IF in the route discovery phase) is directly compared with that of AODV (with flooding in the route discovery phase). In both cases, the node range z is set to 100 m while the node spatial density ρ is set to 2200 nodes/km^2.

In Fig. 3, $\overline{N}_{\mathrm{rtx}}$ is shown, as a function of c, comparing the IF protocol with flooding. The node range z is set to 100 m while the node spatial density ρ is set to 2200 nodes/km^2. As expected, for very high values of c, $\overline{N}_{\mathrm{rtx}}$ with IF converges to the value obtained by flooding. It can be observed that, by setting $c = 0.2$, the iAODV protocol can save roughly 20 rebroadcasts with respect to the AODV protocol, which corresponds to almost 30% of saved retransmissions.

We remark that the reduction of transmitted control messages predicted by the proposed analytical framework is related to a single source node in the first round of propagation: therefore, the total number of saved rebroadcasts in the entire network can be extremely larger, especially considering dense multi-source ad hoc networks. Regarding the second and the following rebroadcast rounds, computing the number of rebroadcasts is much more complicated, since it depends not only by the number of rebroadcasters in the previous rebroadcast round, but also on their specific positions. This is a challenging problem and we are currently working on it. Finally, we remark that the IF strategy mitigates the BSP not only by statistically reducing the number of rebroadcasted packets, as done, for example, in [11], but also by selecting, in an average statistical sense, the best rebroadcaster nodes and adapting itself to the network conditions.

5. Simulation setup

In this section, we detail the simulation set-up behind the performance analysis of the iAODV protocol. In particular, we describe the three relevant and complementary networking scenarios of interest (pedestrian, pedestrian–vehicular, and vehicular) together with the selected performance metrics. All simulations are carried out with the ns-3 (ns-3.19) tool [20]. In all simulated scenarios: the number of nodes in network is denoted by N; each node has the same transmission range z (dimension: [m]); each source node generates packets of dimension P_s (dimension: [byte/pkt]) at a packet generation rate λ (dimension: [pkt/s]). The packets are then transmitted with a fixed data rate (on the wireless channel) $R = 1$ Mbps. The number of source nodes is denoted as N_{tx} and the corresponding destinations are randomly chosen among the set of all nodes. Since unicast transmissions are considered, the number of destinations is at most equal to N_{tx}. In particular, a single node may happen to be the destination for more than one source node.

At the network layer, the performance of iAODV is compared with those of AODV and AODV+G protocols [11]. As already mentioned in Section 2, the AODV+G protocol, embeds a static probabilistic broadcast in the route discovery process of the AODV protocol. In particular, the retransmission probability of the AODV+G protocol is set to $p = 0.65$ [11]. The characteristic control parameters of AODV, AODV+G, and iAODV protocols, outlined in Subsection 4.1, are set as indicated in [1], namely: *hello interval* = 1 s and *allowed hello loss* = 2. For the lower layers, the wireless communication protocol stack defined by the ad-hoc IEEE 802.11b standard is used [21].

5.1. Pedestrian scenario

This kind of scenario is representative for opportunistic ad-hoc networks of smartphones or tablets (namely, social proximity networks [5]). Since nodes correspond to pedestrians, this scenario is characterized by high node spatial density and low node speed. For example, one can imagine an application where a pedestrian may seldom send a very short information packet (e.g., containing his/her position) to intended destinations—for example this position information could be sent periodically, with a relatively long period (because of the low speed of the considered terminals). For the sake of performance analysis, we assume that nodes are uniformly positioned over a square region with side L (dimension: [m]) given by:

$$L = \sqrt{\frac{N}{\rho}} \tag{14}$$

All nodes move according to the mobility model "RandomWayPointMobilityModel," available in ns-3, with speed s_{p} (dimension: [m/s]).

An illustrative example of a pedestrian scenario with $N = 180$ nodes and $\rho = 1700$ nodes/km^2 is shown in Fig. 4. The length of the side of the square region is $L \simeq 325$ m.

5.2. Pedestrian–vehicular scenario

In a pedestrian–vehicular scenario, both vehicles and pedestrians are present, so that a designer has to deal with heterogeneous devices, in terms of both speed and mobility patterns.

We define a scenario constituted by a single road, with two lanes, which surrounds a square region populated by pedestrians. The side of the square region is set as in the pedestrian scenario of Subsection 5.1, i.e., is given by (14). Nodes can be of two types: pedestrian or vehicular. In particular, we assume that N_{ped} pedestrian nodes are positioned randomly in the inner square region and move, without crossing the surrounding roads, with the same mobility model of the pedestrian scenario in Subsection 5.1 (i.e., random way point). The number of vehicles is denoted as N_{veh} and we assume that they are constrained to move along the road in a single driving direction. The ratio $N_{\text{ped}}/N_{\text{veh}}$ is fixed and set to 4—this is realistic for a "popular" square (e.g., a square with touristic attractions). The movement of the vehicles is generated with the SUMO open-source mobility simulator [22] integrated with the ns-3 simulator [23]. SUMO is a road traffic simulator that allows to

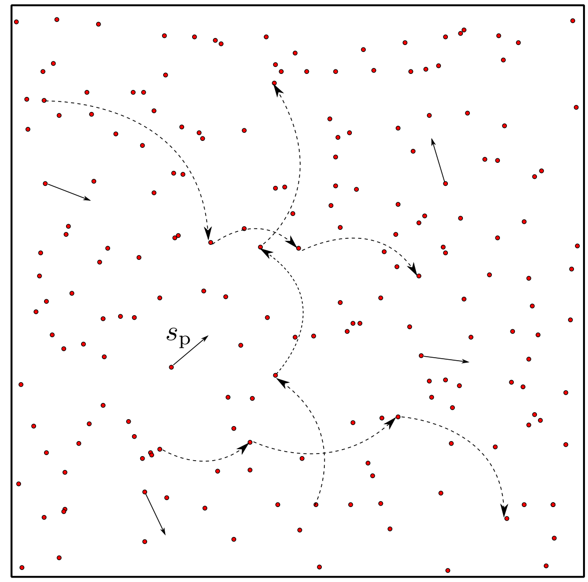

Fig. 4. Illustrative example of pedestrian scenario. $N = 180$ nodes are deployed over a square region with a side $L \simeq 325$ m and a node spatial density $\rho = 1700$ nodes/km^2. For the sake of clarity, we show the speed vector (solid lines with arrows) only for a few representative nodes. Multi-hop paths are represented through dashed lines.

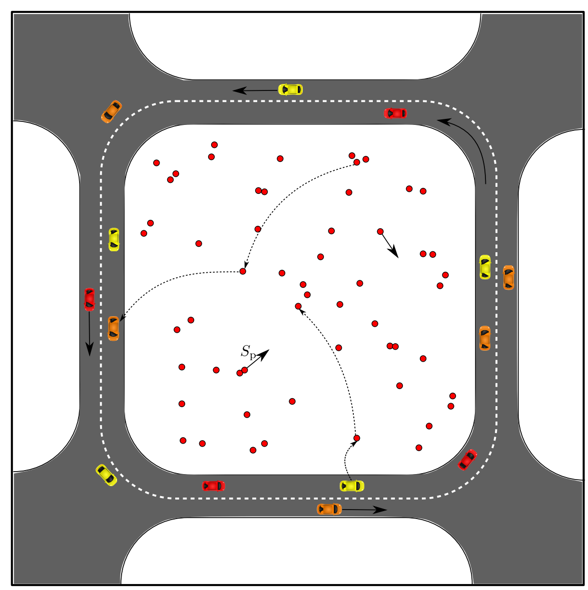

Fig. 5. Illustrative example of *pedestrian–vehicular* scenario. $N_{\text{veh}} = 14$ vehicular nodes are positioned along the road while $N_{\text{ped}} = 56$ pedestrians are positioned into the inner square. For the sake of clarity, we show the speed vector (solid lines with arrows) only for a few representative nodes. Multi-hop paths are represented through dashed lines.

create a vehicular scenario by using one of its external tools or by converting an existing map.

In Fig. 5, an illustrative example of the scenario at hand, with $N_{\text{ped}} = 56$ and $N_{\text{veh}} = 14$, is shown.

5.3. Vehicular scenario

The considered vehicular scenario is representative for the center of a large European city with many road intersections. In this kind of scenario, roads are typically narrow, with a single lane and a single driving direction. Moreover, the nodes' speeds are highly heterogeneous: in fact, although vehicles can move fast, they are

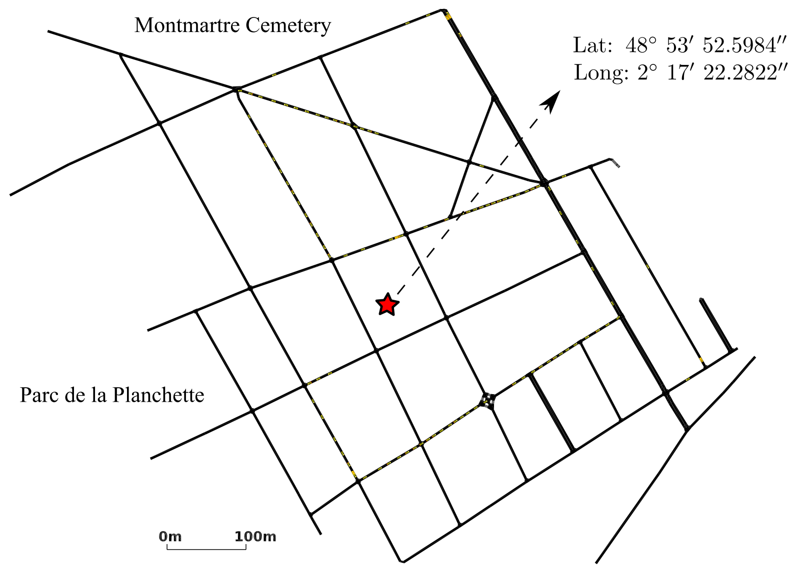

Fig. 6. Illustrative example of VANET scenario: portion of the city center of Paris (namely, the district between "Parc de la Plachette" and the "Montmartre cemetery") imported into the SUMO mobility simulator.

constrained to abide by the traffic rules (priorities, traffic lights, etc.) forming queues and thus slowing down the overall vehicular traffic mobility. Since this highly dynamic mobility can strongly affect the performance of the used routing protocols, realistic VANET mobility models must be taken into account. In the last years, many approaches have been proposed in order to derive realistic mobility models for VANETs [22,24]. In order to simulate realistic vehicular mobility, we exploit the Open Street Maps (OSM) tool [25]. OSM provides open and editable maps of the real world which can be exported into the SUMO format in order to obtain real-world vehicular mobility. Then, by integrating SUMO into ns-3, realistic VANET simulations can be run. As a representative vehicular scenario, we decided to simulate a portion of the city center of Paris (namely the district between "Parc de la Plachette" and the "Montmartre cemetery"), which is shown in Fig. 6.

5.4. Performance metrics

The simulation-based performance analysis is carried out investigating the following metrics: the throughput S (adimensional), the end-to-end delay D (dimension: [s]), the total number of broadcasted packets N_{broad} (dimension: [pkt]), and the average communication distance d_{com} (dimension: [m]). We now shortly describe the considered metrics. The *throughput* is defined as the ratio between the number of packets that reach the intended destinations and all transmitted packets. The *end-to-end delay* is defined as the time during which a single packet stays in the network, from the generation instant (at its source) to the instant at which it reaches its destination. The end-to-end delay is obtained as the average of all per-packet delays. The *total number of broadcasted packets* is given by the sum of the number N_{hello} of hello messages and the number N_{RRREQ} of RREQ packets transmitted during the entire simulation. The *average communication distance* is defined as the distance covered by a single packet, from the source to its final destination, averaged over all successfully delivered packets.

6. Performance analysis

In this section, we explore the simulation-based performance results obtained in the considered networking scenarios: pedestrian, pedestrian–vehicular, and vehicular.

6.1. Simulation results in pedestrian scenarios

In Fig. 7, the performances of AODV, iAODV, and AODV+G protocols, in terms of (a) throughput and (b) delay, as functions of the packet generation rate λ, are directly compared. The main network parameters are set as follows: $P_s = 40$ byte/pkt, $\rho = 1700$ nodes/km^2, $N = 180$ nodes, $N_{\mathrm{tx}} = 40$ nodes, and $s_p = 1.5$ m/s. First of all, it can be observed that the iAODV protocol outperforms AODV and AODV+G protocols for all the considered values of packet generation rate. All the considered protocols reach the so-called saturation condition (in terms of throughput and delay) for large values of λ (namely, $\lambda \geq 40$ pkt/s) [26]. More precisely, the network reaches a saturation regime when each source has always at least one packet in its transmission queue, so that increasing further λ does not change the network conditions and S and D remain approximately constant. The accumulation of packets in the transmission queues occurs for large values of λ also because, when the network load is high, the backoff mechanism of the lower layers (IEEE 802.11b) slows down the transmissions, in order to avoid collisions, as much as possible.

Focusing on Fig. 7(a), it can be observed that using the iAODV protocol, the network reaches the saturation conditions more slowly with respect to the AODV protocol. This is because, for a given value of λ, the iAODV protocol uses a smaller number of RREQ messages, with respect to the AODV protocol, leading to lower channel contention and faster transmissions, which, in turn, reduce the packets' queuing. These observations are confirmed by the delay results, which show that the delay of the iAODV protocol is significantly lower than that of the AODV protocol: this means that a single packet reaches its destination with a smaller number of backoffs, because of limited channel contentions, along the traversed hops.

Note that, in Fig. 7, the performance of the AODV+G protocol is slightly better than, but trend-wise very similar to, that of the AODV protocol. It is worth noting that the AODV+G protocol, although designed to reduce the BSP, is outperformed by the iAODV protocol for all the considered values of λ. This is mainly due to the AODV+G protocol's inability to effectively select the rebroadcaster nodes. By selecting the rebroadcasters in a random manner, the AODV+G protocol leads to the creation of multi-hop routes with a larger number of hops with respect to the iAODV protocol.

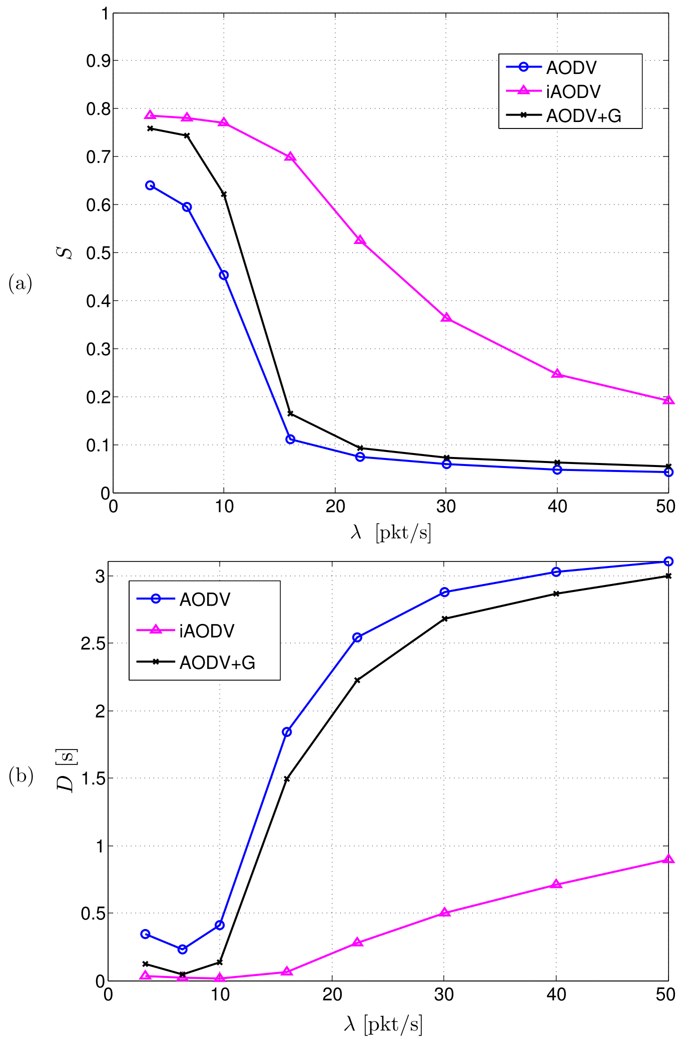

Fig. 7. AODV, iAODV, and AODV+G protocols are directly compared, in terms of (a) throughput and (b) delay as functions of λ, in a *pedestrian scenario*. In all cases: $P_s = 40$ byte/pkt, $\rho = 1700$ node/km^2, $N = 180$ nodes, $N_{tx} = 40$ nodes, and $s_p = 1.5$ m/s.

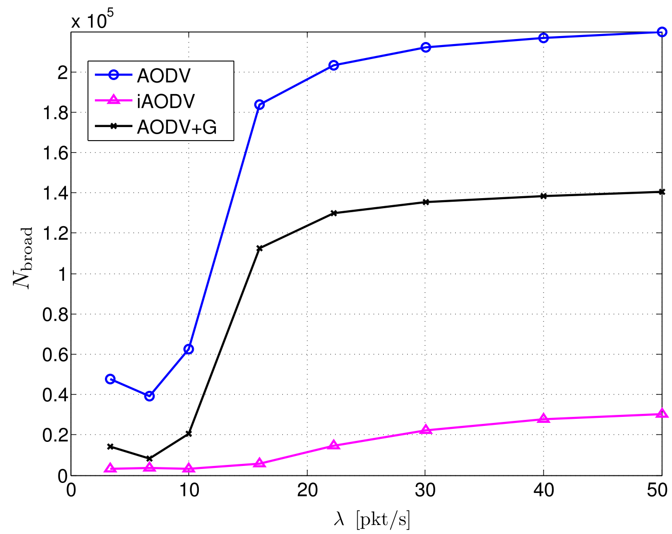

Fig. 8. Total number of broadcasted packets, as functions of λ, in the *pedestrian scenario*. The AODV, iAODV and AODV+G protocols are compared. In all cases: $P_s = 40$ byte/pkt, $\rho = 1700$ nodes/km^2, $N = 180$ nodes, $N_{tx} = 40$ nodes, and $s_p = 1.5$ m/s.

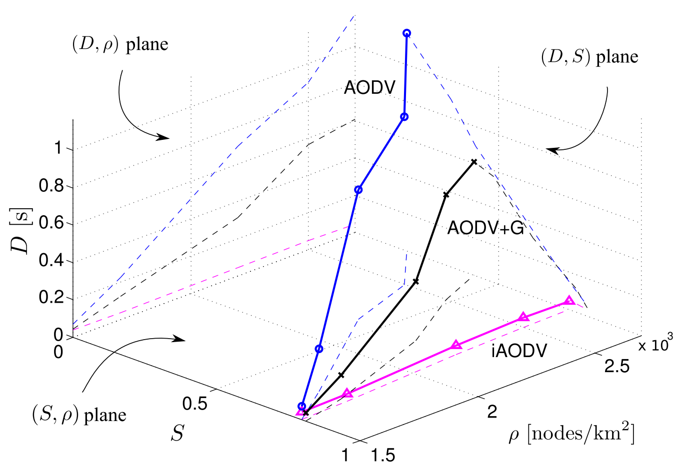

Fig. 9. Three-dimensional characterization of delay and throughput, as functions of ρ, in the *pedestrian scenario*: AODV, iAODV and AODV+G are compared. In all cases: $P_s = 40$ byte/pkt, $\lambda = 3.33$ pkt/s, $N_{tx} = 40$ nodes, and $s_p = 1.5$ m/s.

This, in turn, increases the collision probability and the number of experienced backoffs.

In order to explore the amount of traffic overhead generated by the considered routing protocols in the pedestrian scenario, in Fig. 8 N_{broad} is shown, as a function of λ, in the same conditions of Fig. 7. It can be observed that the use of iAODV significantly limits the number of broadcasted messages, especially in the saturation regime (high traffic load). This leads to a better occupation of the radio channel, thus justifying the global performance improvement observed in Fig. 7. Note that the modifications made in the route discovery process (from AODV to iAODV) do not affect the broadcast of hello messages. However, in this kind of scenario the total number N_{hello} of hello messages is negligible with respect the total number N_{RREQ} of generated RREQ packets.

Focusing on the performance of the AODV+G protocol in Fig. 8, it can be observed that the number of RREQ packets reduces as well, with respect to the AODV protocol, limiting the BSP. However, the iAODV protocol uses a significantly smaller number of RREQ packets than the AODV+G protocol, while still guaranteeing better performance. As already observed, this is due to the fact that the iAODV protocol selects more efficiently the rebroadcaster nodes. For example, for $\lambda = 16$ pkt/s, the AODV+G protocol saves roughly 39% of redundant RREQ packets with $S \simeq 0.17$ (low throughput), while the iAODV protocol can save 90% of rebroadcasts while still guaranteeing $S \simeq 0.7$.

As already said, the IF strategy takes into account the node spatial density. In this way, the overall retransmission probability adapts itself to the network conditions. In order to get more insights about this feature of IF embedded into iAODV, we investigate the impact of the node spatial density on the performance of the considered protocols. The node spatial density is changed by varying the number of nodes and keeping the simulation area (i.e., the side L) fixed. In Fig. 9, a comparative analysis of iAODV, AODV, and AODV+G protocols is carried out in a three-dimensional space, jointly considering node spatial density, throughput, and delay. For each value of ρ, the corresponding values of S and D are computed and the point (ρ, S, D) is drawn for all the considered protocols. The packet generation rate λ is fixed to 3.33 pkt/s and the remaining simulation parameters are set as in Fig. 7. The projections of all curves on all possible planes (namely: (S, ρ), (D, ρ), (D,S)) are also shown.

- The projections on the plane (D, ρ) show that the node spatial density has a negative impact on the delay performance of the

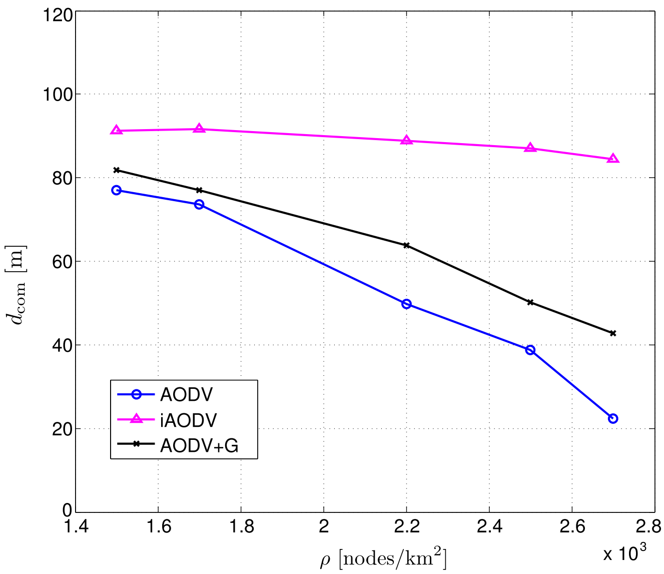

Fig. 10. Average communication distance, as a function of ρ, in the *pedestrian scenario*: AODV, iAODV and AODV+G are compared. In all cases: $P_s = 40$ byte/pkt, $\lambda = 3.33$ pkt/s, $N_{tx} = 40$ nodes, and $s_p = 1.5$ m/s.

AODV protocol. Increasing ρ leads to an increase of the channel contention level, as there are more and more nodes within the transmission range of each other, thus increasing the collision probability. However, it can be observed that the delay of the iAODV protocol is constant with respect to the node spatial density and this proves that IF can adapt effectively its behavior to the network conditions. The performance of the AODV+G protocol lies between those of AODV and iAODV protocols, with a trend similar to that of the AODV protocol.

- Considering the projections on the plane (S, ρ), it can be concluded that the same insights drawn for D are valid also for S. In particular, this performance metric becomes approximately independent of the node spatial density with the use of the iAODV protocol.
- Considering the projections on the plane (D, S), the overall independence of the performance of the iAODV protocol from the node spatial density becomes evident. Conversely, the AODV+G protocol, which limits the BSP in a static manner, cannot adapt itself to the network conditions and its performance degrades for high values of ρ.

In Fig. 10, the average communication distance d_{com} is shown as a function of ρ, in the same conditions of Fig. 9. The more efficient channel utilization brought by IF allows to support longer communication distances. This means that a single packet can be transmitted across multiple hops without being affected by collisions. At the opposite, the route discovery process of the AODV protocol floods the network with RREQ messages, increasing the probability of collisions and reducing the number of successful hops, thus making only destinations close to the source reachable. This aspect becomes more evident for higher node spatial densities (and, correspondingly, channel contention levels). On the contrary, with the iAODV protocol d_{com} seems to be independent of the node spatial density, as already observed in Fig. 9 for S and D. This confirms once more the adaptivity of IF and the corresponding benefits brought by its use in the route discovery phase of iAODV. As already observed before, the performance of the AODV+G protocol is trend-wise similar to that of the AODV protocol, with a performance improvement significantly smaller than that guaranteed by the iAODV protocol.

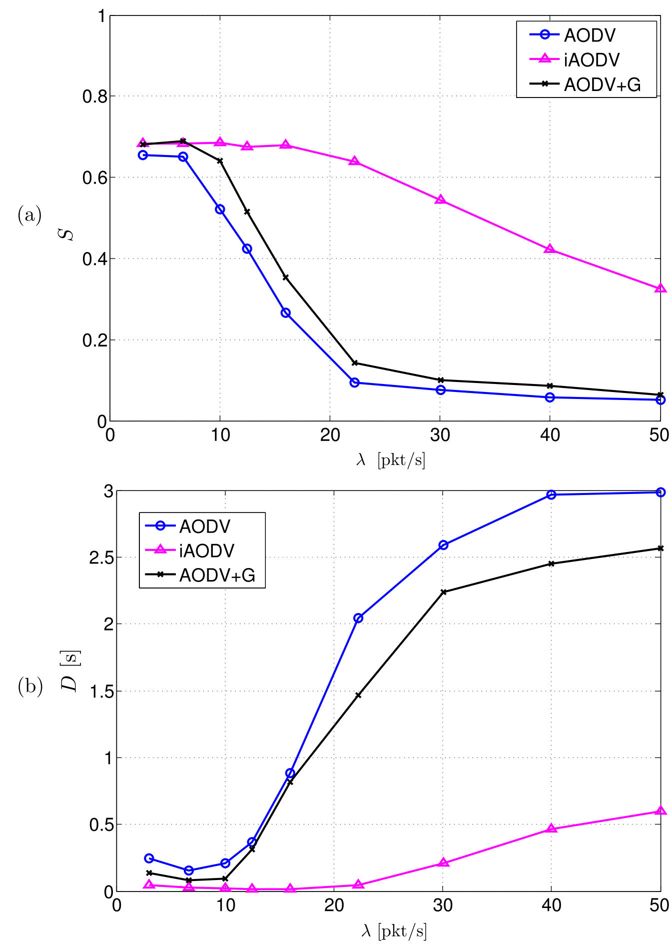

Fig. 11. (a) Throughput and (b) delay, as functions of λ, in the *pedestrian–vehicular scenario*: the AODV, AODV+G and iAODV protocols are compared. In all cases: $N = 160$ nodes, $\rho = 900$ nodes/km^2, $N_{tx} = 30$ nodes, $P_s = 128$ byte/pkt, $s_p = 1.5$ m/s, and $c = 0.3$.

As mentioned in Subsection 5.1, the pedestrian scenario is relevant to an application where pedestrians may send very short data and, in this case, the value of the packet generation rate could be relatively small. In this type of scenario, the obtained results show that the iAODV protocol outperforms the AODV and AODV+G protocols in all considered network conditions, even for medium–low values of λ. For example, with reference to Fig. 7(a) it can be observed that, for $\lambda = 10$ pkt/s, using iAODV leads to a throughput increase, with respect to AODV/AODV+G, of about 73%/26%.

6.2. Simulation results in pedestrian–vehicular scenarios

As anticipated in Subsection 5.2, the pedestrian–vehicular scenario is characterized by the presence of both pedestrians and vehicles. With respect to the pedestrian scenario, we consider smaller values of the number of devices and of the node spatial density—this is expedient to evaluate the efficiency of the iAODV protocol even in sparse networks scenarios. Since, in this scenario, the amount of information to be sent is not necessarily limited, accurate modeling calls for higher values of P_s and λ.

In Fig. 11, (a) the throughput S and (b) the delay D are shown as functions of λ, comparing directly iAODV, AODV, and AODV+G protocols. The main system parameters are set as follows: $N = 160$ nodes, $\rho = 900$ nodes/km^2, $N_{tx} = 30$ nodes, $P_s = 128$ byte/pkt, $s_p = 1.5$ m/s, and $c = 0.3$. Note that the packet generation rate may reach values which are twice the maximum value

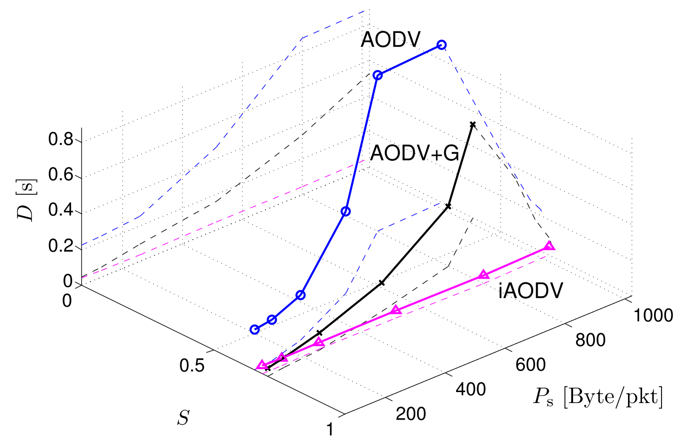

Fig. 12. Three-dimensional (delay, throughput, and P_s) characterization, in the *pedestrian–vehicular scenario*: the AODV, AODV+G, and iAODV protocols are compared. In all cases: $N = 160$ nodes, $\rho = 900$ nodes/km^2, $N_{tx} = 30$ nodes, $\lambda = 4$ pkt/s, $s_p = 1.5$ m/s, and $c = 0.3$.

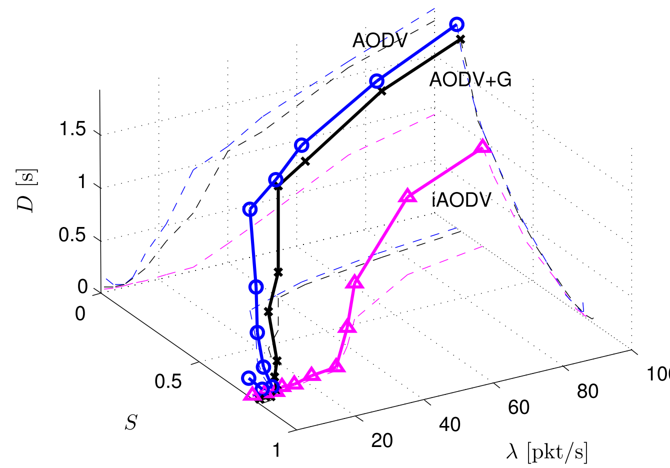

Fig. 13. Three-dimensional characterization of delay and throughput, as functions of λ, in the *vehicular scenario*: the AODV, AODV+G, and iAODV protocols are compared. In all cases: $N = 100$ nodes, $P_s = 128$ byte/pkt, $N_{tx} = 40$ nodes, and $c = 0.3$.

considered in the pedestrian case. Focusing on Fig. 11(a), it can be observed that, for low values of λ, all protocols have roughly the same performance. This is because, with respect to the pedestrian scenario, the values of N and N_{tx} are smaller, and the node spatial density is almost halved. In these conditions, even considering a higher value of P_s, the channel contention is strongly reduced, so that even the flooding strategy, used by AODV in the route discovery process, can perform well. However, for medium–high values of the packet generation rate, the inefficient use of the channel brought by flooding leads the AODV protocol to a fast performance degradation. Focusing on the AODV+G protocol, it can be observed that, even though it outperforms the AODV protocol, it incurs a significant performance degradation for medium–high values of the network load. Conversely, with the iAODV protocol the network does not reach the saturation conditions even for the highest considered values of λ. The delay performance, shown in Fig. 11(b), confirms these conclusions: for low values of λ, all protocols have good performance; for higher values of λ, the delays of the AODV and AODV+G protocols increase, while the delay of the iAODV protocol remains very low.

In addition to the packet generation rate, another parameter that strongly affects the total amount of information sent is the packet size P_s. In Fig. 12, a three dimensional performance analysis is carried out jointly considering D, S, and P_s. The main system parameters are set as in Fig. 11: in particular, the value of λ is set to 4 pkt/s. It can be observed that the iAODV protocol outperforms the AODV protocol for all considered values of P_s. As usual, by focusing on the projections of the curves on the three "side planes," the following insights can be derived.

- From the projection on the plane (D, P_s), it can be observed that increasing the value of the packet size the delay entailed by the AODV protocol explodes. This is due to the fact that with longer packets, a transmission act takes longer, i.e., the channel is "captured" for a longer time. This results in a higher collision probability and leads to network saturation even for low values of λ. However, using the iAODV protocol, the delay does not explode: this is because limiting the number of transmitted RREQ packets saves bandwidth and the channel can thus be used for longer transmissions without the need of a frequent use of the backoff mechanisms.
- From the projection on the plane (S, P_s), it can be observed that an increase of P_s leads, again, to a performance degradation of the AODV protocol. For large values of P_s, the iAODV protocol prevents the network from entering into the saturation regime, thus guaranteeing a better utilization of the radio channel. This makes the throughput of the iAODV protocol to remain almost constant for all the considered values of P_s.
- From the projection on the plane (S, D), it can be observed that the performance of the iAODV protocol is basically independent from P_s. As already observed before, even though the AODV+G protocol outperforms the AODV protocol, its performance does not remain acceptable for increasing values of P_s.

6.3. Simulation results in vehicular scenarios

As anticipated in Subsection 5.3, we consider a vehicular scenario representative of a big city center. In particular, we simulate vehicular traffic in a real portion of the city center of Paris. As mentioned, in such scenario nodes' mobility can strongly affect the performance of a routing protocol. Therefore, accurate modeling is crucial for the evaluation of different vehicular traffic conditions.

In Fig. 13, the performances of the considered routing protocols, in terms of S and D as functions of λ, are shown through a three-dimensional representation. The main system parameters are set as follows: $N = 100$ nodes, $P_s = 128$ byte/pkt, $N_{tx} = 40$ nodes, and $c = 0.3$. It can be observed that the results are quite similar to those obtained in the pedestrian–vehicular scenario (Fig. 11). In particular, while the performances of all protocols are very similar for small values of λ, the iAODV protocol outperforms the AODV and AODV+G protocols for medium–high values of the network load. The reason of this behavior is manly due to the fact that, in the simulated settings, the vehicular scenario includes both vehicles which are free to move and queued vehicles. Therefore, this scenario can be interpreted as a pedestrian–vehicular scenario in which pedestrians correspond to the queued vehicles (almost static).

In order to obtain an exhaustive analysis considering different vehicular traffic conditions, the impact of the number N of vehicles is analyzed. For small values of N, the light traffic conditions allow vehicles to move fast. Conversely, for large values of N the road traffic is congested and the creation of long queues of vehicles slows down the overall vehicular mobility. In Fig. 14, the performances of the considered routing protocols, in terms of (a) throughput and (b) delay, as functions of N, are shown. The main network parameters are set as follows: $\lambda = 12$ pkt/s, $P_s = 128$ byte/pkt, and $c = 0.3$. Regarding N_{tx}, we keep the ratio N_{tx}/N constant and equal to 2/3. It can be observed that, for

(a)

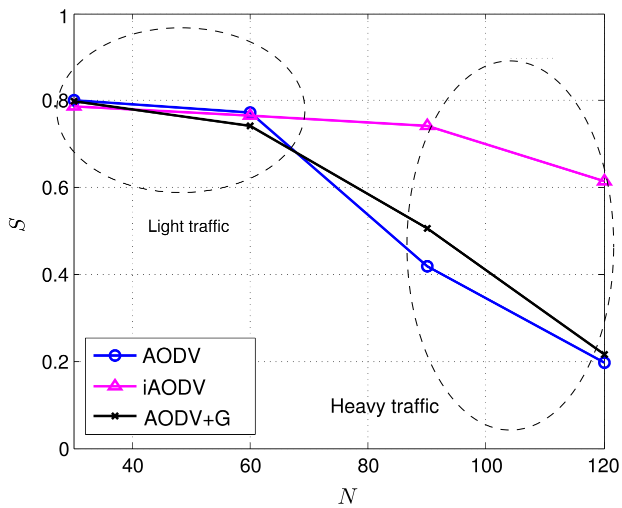

(b)

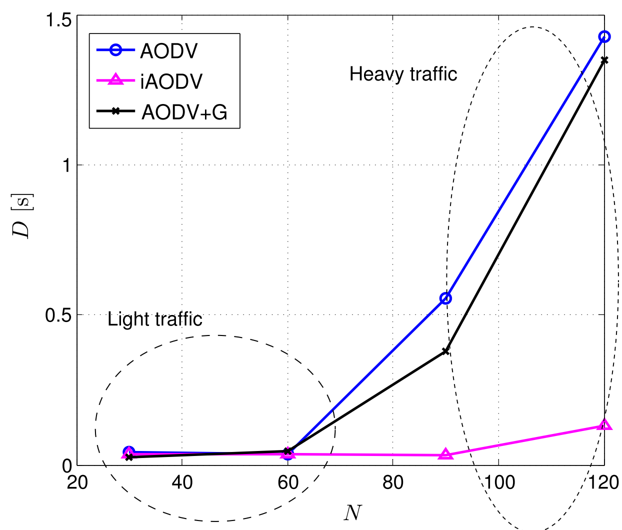

Fig. 14. (a) Throughput and (b) delay, as functions of N, in the *vehicular scenario*. The AODV, AODV+G, iAODV protocols are directly compared. In all cases: $\lambda = 12$ pkt/s, $P_s = 128$ byte/pkt, $N_{tx} = 2N/3$, and $c = 0.3$.

light road traffic conditions, all routing protocols have a similar performance in terms of both S and D. When the vehicular traffic is light, there are no queued vehicles, and the node spatial density reduces: the AODV protocol can thus perform well since the channel contention level is quite low. However, for increasing values of N, vehicular traffic congestion corresponds to a significant increase of the node spatial density and the available bandwidth thus reduces: the wasteful use, caused by flooding, of the radio channel degrades the performance of the AODV protocol. As already observed in the previously analyzed scenarios, the AODV+G protocol cannot guarantee a high performance for increasing values of the node spatial density. Conversely, the iAODV protocol, by effectively adapting itself to the network conditions, guarantees a good performance, in terms of S and D, even in heavy road traffic conditions.

7. Conclusions

In this paper, we have proposed a novel reactive routing protocol, denoted as iAODV, derived from the AODV protocol by replacing the flooding mechanism used in its route discovery phase with the probabilistic forwarding mechanism denoted as IF. Three scenarios have been considered: the first one is representative of a pedestrian ad hoc network; the second is representative of a pedestrian–vehicular scenario which involves both vehicles and pedestrian nodes; the third is a vehicular scenario corresponding to a real portion of the city center of Paris. In all cases, and for almost all the considered values of the network parameters, the iAODV protocol outperforms the AODV protocol and the AODV+G protocol. This is mainly due to the fact that the number of control messages is effectively reduced by the use of IF, thus reducing the contention level and making the channel utilization more efficient.

We remark that the proposed IF-based route discovery process can be applied to any reactive routing protocol which shares the same route discovery phase of the AODV protocol, e.g., the DSR protocol. This represents an interesting research extension of the current work.

References

[1] C. Perkins, E. Royer, Ad-hoc on-demand distance vector routing, in: Second IEEE Workshop on Mobile Computing Systems and Applications WMCSA, New Orleans, LA, USA, February 1999, pp. 90–100.

[2] S. Panichpapiboon, G. Ferrari, Irresponsible forwarding, in: 8th International Conference on Intelligent Transport System Telecommunication (ITST), Phuket, Thailand, 2008, pp. 311–316.

[3] J.-P. Vasseur, A. Dunkels, Interconnecting Smart Objects with IP - The Next Internet, Morgan Kaufmann, 2010, http://TheNextInternet.org/.

[4] O. Abedi, M. Fathy, J. Taghiloo, Enhancing AODV routing protocol using mobility parameters in VANET, in: IEEE/ACS International Conference on Computer Systems and Applications (AICCSA), Doha, Qatar, 2008, pp. 229–235.

[5] L. Pelusi, A. Passarella, M. Conti, Opportunistic networking: data forwarding in disconnected mobile ad hoc networks, IEEE Commun. Mag. 44 (11) (2006) 134–141.

[6] S. Das, C. Perkins, E. Royer, Performance comparison of two on-demand routing protocols for ad hoc networks, in: Proceedings of the 19th IEEE INFOCOM, Tel Aviv, Israel, vol. 1, 2000, pp. 3–12.

[7] A. Tuteja, R. Gujral, S. Thalia, Comparative performance analysis of DSDV, AODV and DSR routing protocols in MANET using ns-2, in: Proceedings of International Conference on Advances in Computer Engineering (ACE), Bangalore, Karnataka, India, 2010, pp. 330–333.

[8] Y.H.D. Johnson, D. Maltz, The dynamic source routing protocol (DSR) for mobile ad hoc networks, http://tools.ietf.org/html/rfc4728.

[9] Y.-C. Tseng, S.-Y. Ni, Y.-S. Chen, J.-P. Sheu, The broadcast storm problem in a mobile ad hoc network, Wirel. Netw. 8 (2002) 153–167.

[10] Y. Sasson, D. Cavin, A. Schiper, Probabilistic broadcast for flooding in wireless mobile ad hoc networks, in: Proceedings of Wireless Communications and Networking, in: WCNC, vol. 2, 2003, pp. 1124–1130.

[11] Z.J. Haas, J.Y. Halpern, L. Li, Gossip-based ad hoc routing, IEEE/ACM Trans. Netw. 14 (2006) 479–491.

[12] A. Aharony, D. Stauffer, Introduction to Percolation Theory, Taylor and Francis, London, 1994.

[13] C.-C. Shen, Z. Huang, C. Jaikaeo, Directional broadcast for mobile ad hoc networks with percolation theory, IEEE Trans. Mob. Comput. 5 (2006) 317–332.

[14] J.E. Wieselthier, G.D. Nguyen, A. Ephremides, Energy-efficient broadcast and multicast trees in wireless networks, Mob. Netw. Appl. 7 (2002) 481–492.

[15] B.S. Mergen, S. Member, A. Scaglione, G. Mergen, Asymptotic analysis of multistage cooperative broadcast in wireless networks, IEEE Trans. Inf. Theory 52 (2006) 2531–2550.

[16] S. Busanelli, G. Ferrari, S. Panichpapiboon, Efficient broadcasting in IEEE 802.11 networks through Irresponsible Forwarding, in: IEEE Global Telecommunications Conference, Honolulu, Hawaii, USA, 2009, pp. 1–6.

[17] A.U. Shankar, C. Alaettinoglu, K. Dussa-Zieger, I. Matta, Transient and steady-state performance of routing protocols: distance-vector versus link-state, Internetwork. Res. Exp. 6 (1996).

[18] C.E. Perkins, P. Bhagwat, Highly dynamic destination-sequenced distance-vector routing (DSDV) for mobile computers, Comput. Commun. Rev. 24 (1994) 234–244.

[19] A. Papoulis, Probability, Random Variables and Stochastic Processes, 3rd edition, McGraw-Hill Companies, 1991.

[20] A. Wang, W. Jiang, Research of teaching on network course based on ns-3, in: First International Workshop on Education Technology and Computer Science, 2009.

[21] WangInstitute of Electrical and Electronics Engineers, IEEE Std 802.11TM-2007. Part 11: Wireless LAN Medium Access Control (MAC) and Physical Layer (PHY) specifications, 2007.

[22] F. Karnadi, Z.H. Mo, K. chan Lan, Rapid generation of realistic mobility models for VANET, in: IEEE Wireless Communications and Networking Conference (WCNC), Hong Kong, China, 2007, pp. 2506–2511.

[23] Chitraxi Raj, Urvik Upadhayaya, Twinkle Makwana, Payal Mahida, Simulation of VANET using ns-3 and SUMO, Int. J. Adv. Res. Comput. Sci. Softw. Eng. 4 (2014) 563–569.

[24] C. Sommer, F. Dressler, Progressing toward realistic mobility models in VANET simulations, IEEE Commun. Mag. 46 (11) (2008) 132–137.

[25] M. Haklay, P. Weber, Openstreetmap: user-generated street maps, IEEE Pervasive Comput. 7 (4) (2008) 12–18.

[26] J. Robinson, T. Randhawa, Saturation throughput analysis of IEEE 802.11e enhanced distributed coordination function, IEEE J. Sel. Areas Commun. 22 (2004) 917–928.